Journal of Electrical Engineering and Automation (ISSN: 2582-3051)
www.irojournals.com/iroeea/

Recent Advances for DC-DC Converter Topology in Hybrid Renewable Energy System

C. H. Sathish[1], I. A. Chidambaram[2], M. Manikandan[3]

[1,2]Department of Electrical Engineering, Annamalai University, Tamilnadu, India
[3]Department of Electrical Engineering, Jyothismathi Institute of Technology and science, India

E-mail: [1]anusmin2@gmail.com, [2]driacdm@gmail.com, [3]cm.manikandan@gmail.com

Abstract

The hybrid renewable energy systems are widely employed to meet the load demand at various critical times. This paper proposes the modelling, simulation, and conversion of energy using multiple power electronic based DC-DC converter topologies in Hybrid Renewable Energy System (HRES) which consist of solar and wind turbine energy sources, for enhancing the system stability and efficiency. This work presents a novel high gain power electronic DC-DC known as Modified Single-Ended Primary-Inductor Converter with magnetic coupling for boosting voltage in HRES. Landsman converter is used to reach peak DC output voltage, improve power quality and voltage stability, reduce conversion of power stages, and decrease losses compared to the present power electronic converter coupled with HRES. Moreover, adaptive neuro fuzzy system controller is proposed in this research to gain peak power from photovoltaic system. The results are validated using SIMULINK/MATLAB software.

Keywords: Adaptive neuro fuzzy system, landsman converter, hybrid renewable energy system, modified single-ended primary-inductor converter

Abbreviations

ANFIS	Adaptive Nero-Fuzzy Inference System	LC	Inductor Capacitor
WT	Wind Turbine	P-O	Perturb-Observe
WECS	Wind Energy Conversion System	PV system	Photovoltaic system
MW	Mega Watt	CCM	Continuous Current in Conduction Mode
IG	Induction Generators	SEPIC	Single Ended Primary Inductance Converter
GW	Giga watt	DFIG	Double Fed Induction Generator
IC	Incremental Conductance	L Converter	Landsman Converter
WT	Wind Turbine	RB controller	Rule Base Controller
MPPT	Maximum Power Point Tracking	EST	Energy Storage Technology
RES	Renewable Energy Source	M-SEPIC	Modified Single-Ended Primary-Inductor Converter

DOI: https://doi.org/10.36548/jeea.2022.4.005
Received: 19.10.2022, received in revised form: 25.11.2022, accepted: 07.12.2022, published: 17.12.2022

1. Introduction

In recent era, to meet the demand of load, the remnant fuels are comprehensively used up which cause their depletion. The use of fossil fuels contributes to the occurrence of global warming. The best option for supplying green energy to solve this global energy catastrophe is renewable energy sources. In FW2021, India had 94.5GW renewable energy capacity, and 152.36 GW of installed renewable energy competence as of January 2022. In January 2022, there was an augment in the renewable energy capacity of 975.60 MW. The percentage of installed electricity capacity that comes from non-fossil sources as of January 2022 is 38.56 percent, which is in line with the ambition of 40 percent by the end of 2022. By 2030, the nation hopes to have 500GW of renewable energy installation, with solar power accounting for 300GW (more than 60%) [1].

The creation of the majority of renewable energy sources, such as photovoltaic system and wind turbine system, is known to be significantly intolerant by the neighboring environment. As a result, output characteristics that are unstable are created, which is the primary drawback of renewable energy invention. The nation's industrial development and economic condition are being hampered by the energy crisis, which is the primary driver behind the switch to Renewable Energy Sources (RES). The demand for electrical energy has been rising endlessly as a result of the industrial revolution. Additionally, the usage of conservative fossil fuel technologies harms the environment by releasing greenhouse gases like CO_2. As a result, RES like wind, solar, biomass, hydroelectricity, etc. have come into focus. The most popular renewable sources that are regularly used for generating supply are solar and wind energy. The RES not only offers energy free of cost but also energy that is clean [2, 3]. In any case, there are occasions when, relying only on a specific RES fails to provide the obligatory grid electricity. Grid-connected mode and islanding mode are the two operational modes for Hybrid Renewable Energy System (HRES), each with their own advantages and disadvantages. The islanding mode is advantageous in places where grid connections are impractical, and it helps electrify places where it is demanding to build transmission lines. Grid-connected mode is favorable in locations with established transmission lines and a need for dependable supply, such as cities and towns [4].

Photovoltaic energy is typically documented as a significant renewable energy due to its widespread availability, low cost, and lack of pollutants. PV technology is the process of employing semiconductors to turn solar energy into electrical current [5, 6]. Before being fed into the grid, the less value of DC voltage generated by photovoltaic is increased. A

transformer is frequently used to increase voltage gain. However, because it is heavy and expensive, the usage of transformers has been constrained [7]. To increase the output energy of PV system DC-DC converter with high gain is used [8, 9]. Based on the voltages and currents employed, micro grids can be roughly divided into AC, DC, and hybrid micro grids.

A DC-DC converter is thought future essential for converting the low voltage to a high voltage because the voltage output from a PV is essentially a low DC voltage and it changes with the changing weather and solar irradiation [10]. In terms of DC-DC converters, boost converters are employed to raise the voltage of PV panels, and their integration lowers the input ripple current from the solar panel, boosting the panel's dependability and extraction power. Despite these advantages, boost converters require more switching devices due to their discontinuous input and output. As a result, the gain of the circuit fluctuates, which affects the dynamics of the circuit. A buck-boost converter has been created that has a broad input and output voltage range and improved performance to get around this restriction. The DC input voltage range is expanded thanks to an extra input function, considerably enhancing the adaptability of the PV panel while maintaining centralized operation.

In PV systems with reduced ripple current and better voltage gain, zeta converters are also used, although the voltage gain is sensible due to inductance leakage. The PV panel's CUK converters demonstrated low switching losses, improved voltage control, and higher efficiency for flexible operation. However, these converters slowed slowly, affecting the exact usage, as a result of the sudden speed up/down voltage that resulted. Furthermore, the CUK converter can only operate in the medium-low power range since high-power operation requires large input and output inductors, and the converter suffers damage from utility grid voltage swings when connected to it. Additionally, SEPIC converters are used in PV systems to produce a non-inverting output that is thought to be simple to drive due to the referenced switch towards the ground node. These converters are not better, nevertheless, in terms of price and effectiveness. The Landsman converter, which provides noiseless operation and increased efficiency, is used to address these problems. Many DC-DC converters, including boost, buck-boost, KY, SEPIC, and others, are used with the PV system to carry out an effective DC-DC conversion process. The decrease of Total Harmonic Distortion (THD), settling time, peak overshoot difficulties, and steady state error using successful control approaches considerably increases the converter's efficiency [11].

In this study, to enhance output voltage of PV system, a high gain DC-DC boost converter is designed. However, the PV system's inconsistent behavior, instability, and

subpar conversion capacity have an impact on its presentation. The PV system must therefore use a DC-DC converter along with MPPT method to guarantee that it generates the most power possible [12]. To make the most of the power generated by the PV panel, a number of power tracking techniques are in use. The solar isolation, temperature of cell, and load linked to the PV panel are the essential factors that affect how much power it produces. All these elements have an impact on how creative the PV system is. In order to obtain the best level of efficiency for PV frameworks, an effective MPPT algorithm is applied. Incremental conductance, hill climbing, open circuit voltage, ripple correlation control are some of the traditional MPPT approaches that are initially taken into consideration. These MPPT techniques, however, are ineffectual because they result in peak overshoot issues and output oscillation [12]–[14]. Therefore, an MPPT algorithm based on Artificial Intelligence (AI) such as ANFIS based MPPT method is used to address these problems.

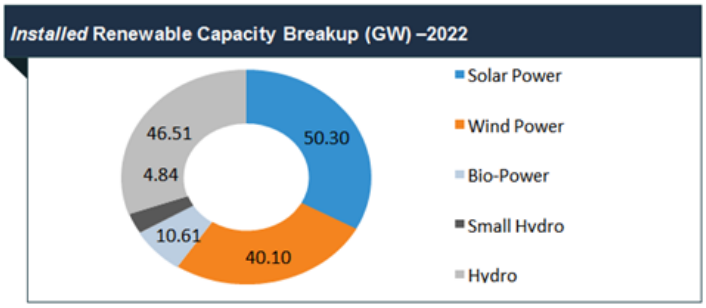

Figure 1. Installed Renewable Energy Capacity [1]

On the other hand, wind energy is a rapidly expanding RES that uses wind energy to produce electricity [15]. The two most popular types of wind turbine generators are synchronous generators and Induction Generators (IG). Because induction generators are dependable, affordable, straightforward, strong, and have a high rotational speed, they are used in this task. In the past, constant speed IGs was used to power wind turbines in small capacity systems. Employing this constant speed passive output limitations are what keep IGs in their place [16, 17]. Double Fed Induction Generators (DFIGs) are now regarded as a viable solution for achieving variable speeds after a number of years. The speed and efficiency of the wind energy system are further increased by its low cost and straight forward design [18, 19]. Energy storage technology is applied here to reduce power fluctuations brought on by unstable RESs like wind, solar, etc. Consequently, the battery's function is to enhance the eminence and stability of electrical power before it is transmitted to the load [20, 21]. The converter must be isolated in order to manage how the battery operates. There is no reference voltage, which isolates DC converters with isolated voltage issues. Trying to decrease the grid voltage causes issues.

2. Proposed System Description

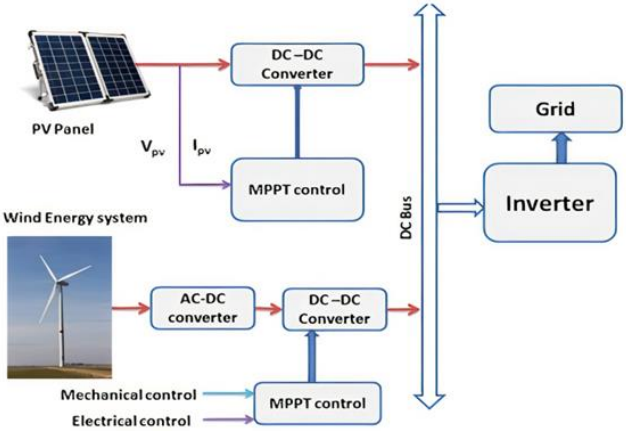

Figure 2. Proposed Hybrid Renewable Energy System

The proposal of an L-converter in a hybrid renewable energy system is the work's originality, and the focus of the research in this article is on the problems of HRESs. The grid linked DC-DC converter is not isolated, has fewer power conversion stages, and has less loss than contemporary hybrid grid-connected systems. The SEPIC converter continuously generates input current, minimizes input ripple current, and alleviates output voltage stress. The L-Converter and the PV system's output side work together to increase output voltage while minimizing switching loss. Numerous power converters and management systems are designed for managing and monitoring active and reactive power because renewable energy sources are intermittent.

The primary aim of this proposed work is the modeling of hybrid renewable energy system using PV system with wind turbine system to generate a stable and peak power during various abnormal electrical behaviors like voltage imbalance, swells, harmonic distortions, notching, sags, transients, etc. The energy produced by solar and wind energy is supplied through a DC to DC converter before being transferred to an inverter circuit, where the semiconductor devices in the circuit are given gate pulses by a PWM system. In the Wind Energy Conversion System (WECS), the wind turbine converts the kinetic energy of the turbine into mechanical energy, and the Double Fed Induction Generator converts mechanical energy obtained from wind turbine into electrical energy in the alternative nature. Hence, a PWM rectifier is used here to convert the AC voltage into DC voltage.

2.1 Solar PV Modelling

The solar cell is the most essential component of a PV system that generates DC voltage when exposed to sun light based on the phenomenon of photovoltaic effect. A PV

panel consists of many solar cells, which are linked inparallel and series, with the expansion of parallel connection increasing the current and the expansion of series connection increasing the voltage. A PV array is made up of many PV panels. Figure 3 illustrates the PV cell equivalent circuit.

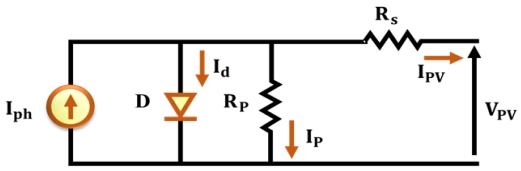

Figure 3. PV cell equivalent circuit

By applying Kirchchoff's current law,

$$I_{PV} = I_{Ph} - I_d - I_P \tag{1}$$

$$I_d = I_o \left[\exp\left(\frac{V_{PV} + I_{PV} R_S}{nv} \right) - 1 \right] \tag{2}$$

Here,

$$I_p = \left(\frac{V_{PV} + I_{PV} R_S}{R_P} \right) \tag{3}$$

$$I_{PV} = I_{ph} - I_o \left[\exp\left(\frac{V_{PV} + I_{PV} R_S}{nv} \right) - 1 \right] - \frac{V_{PV} + I_{PV} R_S}{R_P} \tag{4}$$

$$V_{OC} = \frac{akT}{q} Log_n \left(\frac{I_{Ph}}{I_d} + 1 \right) \tag{5}$$

$$V_{OC} = \frac{akT}{q} Log_n \left(\frac{I_{Ph}}{I_d} + 1 \right) \tag{6}$$

Here, I_{PV} specifies the PV output current that flows through the series resistance R_S, V_{PV} specifies the PV output voltage , I_{ph} specifies the photo generated current, I_d specifies the diode saturation current, I_P specifies the current that flows through the shunt resistance R_P, n stands for number of series connected solar PV cells, v represents the junction thermal voltage, a stands for diode ideality constant, q represents the electron charge, which has a value of $(1.602 \times 10^{-19} C)$, k denotes the Boltzmann constant $(1.381 \times 10^{-23} J/K)$ and T denotes PN junction temperature.

2.2 Modeling of Wind Turbine

Wind turbine generation power output is given as,

$$p_{wg} = \begin{cases} p_{rp}\left(\dfrac{v_{WT}^{2} - v_{c}^{2}}{v_{r}^{2} - v_{c}^{2}}\right), v_{c} \le v_{WT} \le v_{r} \\ p_{rp}, v_{c} \le v_{WT} \le v_{fc} \\ 0, v_{WT} \ge v_{fc} \end{cases} \quad (7)$$

Where, P_{Wg} is wind generator output power, p_{rp} is wind generator rated power, v_c is WT cut speed, v_r is WT rated speed, and v_{fc} is cut speed rotation of wind turbine stops.

$$V_{hwT} = v_{ref}\left(\frac{H}{H_{refWT}}\right)^{\alpha} \alpha \quad (8)$$

Here, V_{hWT} is the Turbine height wind speed (H), v_{refwT} is wind speed noted by meteorological station at height (H_{ref}), α is the Roughness Surface factor which is approximately equal to 1/7in of an open surface of space.

PMSG wind turbine Mechanical Wind Power,

$$P_M = \frac{1}{2}\rho A V_w C_P(\lambda, \beta) \quad (9)$$

Here, $\lambda = \dfrac{rwm}{v}$, r is the turbine of wind surface, wm is the shaft speed angle of turbine, and v is the wind velocity.

By considering betz limit, the experimental maximum power efficiency 0.59 is for WT system. This is known as power coefficient and is given as,

$$c_{p\max} = 0.59, c_p = \frac{p_r}{p} \quad (10)$$

Where, $P_{r,}$ is the extracted power (available power), P_M is the mechanical output power of the turbine (w), ρ is the air density in kg/m^2, A is the swept area of Turbine m^2, V_w is wind speed (m/s), C_P is the performance coefficient of the wind turbine, λ is the tip speed: it is ratio of the rotor blade tip speed to wind speed, and β is the blade pitch angle. When transferring WES-generated power to the utility, back-to-back power electronic converters are frequently suggested to meet power quality requirements.

3. PV Coupled DC-DC Converter

3.1 M- SEPIC converter model

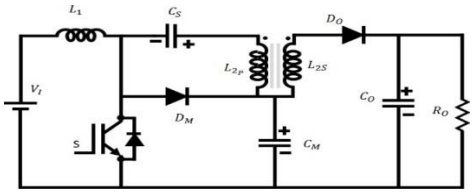

Figure 4. M-SEPIC converter

The modified SEPIC converter is used as magnetic and without magnetic coupling. With magnetic combination, it enhances the static gain and switching voltage at a very low level. The M-SEPIC converter essentially uses a boost converter after that, by buck-boost converter, although it has more advantages of having non-inverted response. By using renewable sources, M-SEPIC converter without magnetic combination can perform twice of the static gain of the boost converter for a high duty cycle operation. But a practical drawback of M-SEPIC converter in order to keep the duty cycle of converter close to D=0.86 is that it results in peak static gain identical to approximately q=12.5. An easy answer to elevate static gain without enhancing the duty cycle and the switch voltage, is to take in an inductor L_2 in the secondary winding. The output of the secondary winding increases with the help of inductor winding turn ratio N. This converter produces problem of high voltage at the output of diode D_O due to existence of leakage inductance of L_2 in the coupling winding. The output diode reverse recovery current causes the energy stored in leakage inductance, and results in voltage sphere and peak reverse voltage at the diode output D_0. It is difficult to control this overvoltage with snubber or clamping circuits. To overcome this effect is to include voltage multiplier at the secondary side. This voltage multiplier boosts the converter static gain and production voltage, works in CCM with output diode clamping. Here all capacitors taken are as voltage sources and for theoretical concern all semiconductors are ideal.

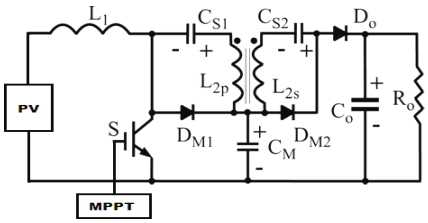

Figure 5. Mode 1 operation

Mode 1: [t_0-t_1] The switch S is ON and input inductor L_1 reserves the energy. The C_{S2} is charged by $L_{2S,}$ DM2. The leakage inductance limits the current. The output diode is impassable, and the peak diode voltage becomes identical to (v_0-v_{cm}), and the energy transfers to the capacitor C_{S2} at the instant t_1.

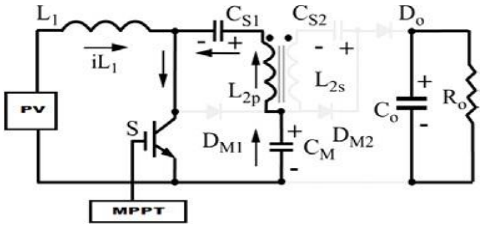

Figure 6. Mode 2 operation

Mode 2: [t_1-t_2] Dm2 is blocked at instant t_1 and the switch is off, the inductors L_1, L2 store energy, and the current linearly increases at the instant t_2.

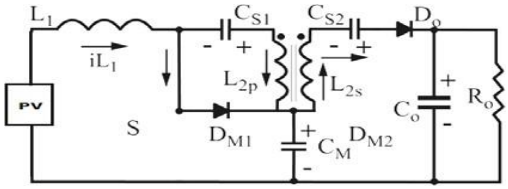

Figure 7. Mode 3 operation

Mode 3: [t_2-t_3] The inductor L_1 stores energy and transfers to Capacitor C_M. C_{S1}, CS2, L2 and D_0 receive energy through output.

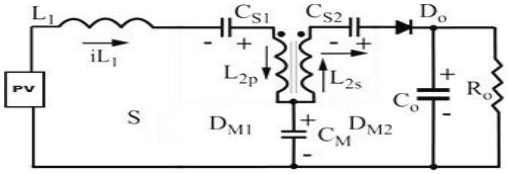

Figure 8. Mode 4 operation

Mode 4: [t_3-t_4] While the power switch is turned on, the energy shifting to the output is preserved at the spot t_4.

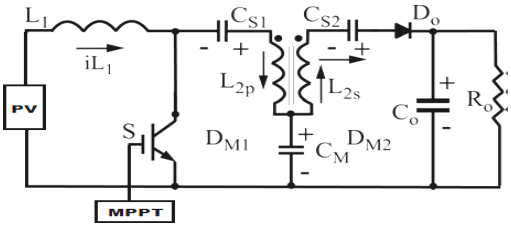

Figure 9. Mode 5 operation

Mode 5: [t_4-t_5] When the switch is going on at moment t_4, D_o current decreases linearly and transformer leakage inductance restricts the di/dt. Decreasing the diode current, recovers problems.

The M-SEPIC converters with magnetic combination and with voltage multiplier of secondary side theoretical wave forms are described in fig. 10. M-SEPIC converter magnetic combination and voltage multiplier static gain can be calculated by,

$$\frac{v_o}{v_i} = \frac{1}{(1-D)}(1+N) \tag{11}$$

The N winding turn ratio increases static gain without increasing switching voltage.

$$N = \frac{N_{L2S}}{N_{L2P}} \tag{12}$$

N is the winding turn ratio of the inductor. The duty cycle is given by,

$$D = 1 - \frac{V_{in}}{V_0}(1+N) \tag{13}$$

The switch and diode voltage are given as,

$$V_S = V_{Dm1} = \frac{V_{in}}{(1-D)} \tag{14}$$

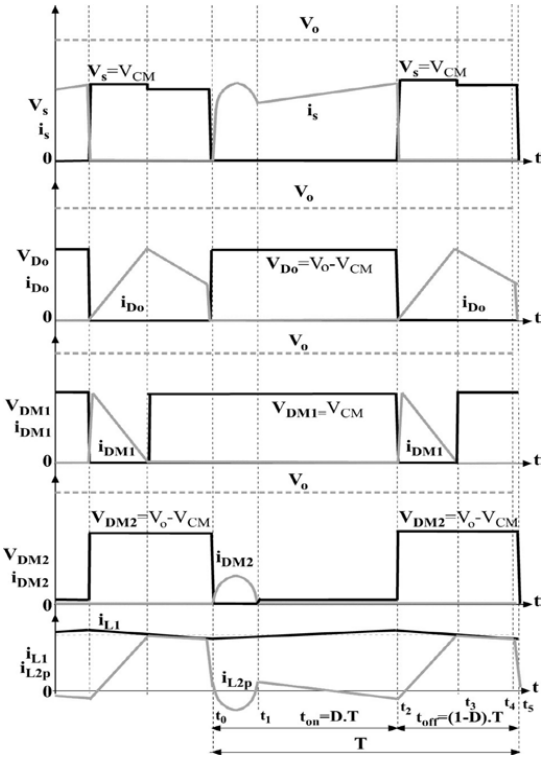

Figure 10. Theoretical wave forms

The diodes Dm^2 and D_o $_{Dm2}$ and produce same voltage. This is given as,

$$V_{D_o} = V_{Dm2} = V_O - V_{cm} = N\frac{V_{in}}{(1-D)} \tag{15}$$

The value of inductance L_1 is given as,

$$L_1 = L_{2p} = N\frac{(V_{in} \times D)}{(1-D)} L_{2S} = N^2 \times L_{2P} \tag{16}$$

3.2 L-converter model

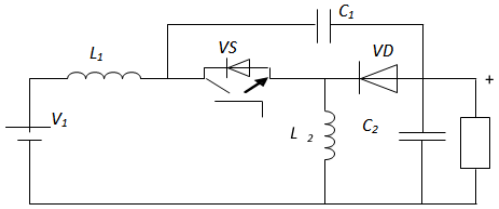

Figure 11. L-Converter

L-converter is a DC-DC converter that enhances the output voltage of PV system. It operates in continuous conduction mode without considering the irradiance level. Fig .11 shows the proposed L-Converter diagram. The excitation and response voltage are given by V_1 and V_2. The switch V_S and response resistance R_O, the current flowing through inductors I_{L1} and I_{L2}, and the voltage across C_1 are in continuous mode. The converter 1 has the capacity to enhance the output voltage when the value of the duty ratio is equal and more than 50%.

Working stage 1: In stage 1, the V_S is turned on and the capacitor voltage V_{C1} causes the diode to reverse bias. Along the switch, a current known as I_{L2} causes L_2 flows. C1 discharges through the switch, shifting energy to the L_2 inductor and the output, because V_{C1} is greater than the response voltage V_O. As a result, VC1 decreases, the I_{L2} rises, and the input provides energy to the input inductor L_1.

Working stage 2: In stage 2, the switch is in off position. Now the diode is in forward bias mode. The current flowing through inductor L_2 becomes I_{L2} flows through diode V_D. The inductor L2 shifts its energy backup to output across the diode; similarly, C_1 is charged over the diode. C_1 is charged across the diode with the energy of V_1 in addition to L_1, thus V_{C1} increases whereas I_{L2} decreases.

The input ripple in current I_{L1} is intended by taking into account the flow of all the ripple components of L_1 across C_1. $\Delta\phi$ represents the additional flux, and the max-to-max ripple current is given by:

$$\Delta I_{L1} = \frac{\Delta \phi}{L_1} \tag{17}$$

At turn off condition, the current is across C_a.

$$I_{c1} = I_{L1} = C_1 . \frac{\Delta V_{c1}}{(1 - D) t_s} \tag{18}$$

Where, D is duty ratio and t_s switching period. The voltage ripple content of V_{c1} is given as,

$$\Delta V_{c1} = \frac{I_{L1}(1-D)t_s}{C_1} \tag{19}$$

$$\Delta I_{L1} = \frac{I_{L1}(1-D)}{8L_1C_1f_{sw}^2} \tag{20}$$

Where, $f_{sw} = \frac{1}{t_s}$ is the switching frequency

$$I_{L1} = \frac{D}{(1-D)I_0} \tag{21}$$

Where, Io is the output current.

$$L1 = \frac{I_o D}{8C_1 f_{sw}^2 \Delta I_{L1}1} \tag{22}$$

The leakage inductance is,

$$L_r = \frac{v_{in}}{(1-D)\frac{di}{dt}.\mathrm{N}}, Where, \frac{di}{dt}\frac{v_{in}}{(1-D)L_r.\mathrm{N}} \tag{23}$$

The resonance period at mode 1 is,

$$T_{res} = \pi\sqrt{L_r\left(\frac{c_{s1}c_{s2}}{c_{s1}+c_{s2}}\right)} \tag{24}$$

Capacitors C_s and C_M can be determined by,

$$c_{s1} = C_m = \frac{I_O.N}{\Delta V_C.f} \tag{25}$$

Where, I_O is the semiconductor current effort, and ΔV_C is the capacitor ripple voltage.

3.3 Modeling of MPPT controller

The adaptable intelligent control method known as ANFIS, developed by Jang in 1993, combines the ANN and the Fuzzy Inference System (FIS). ANFIS converts a system into if-then rules to deal with non-linear functions. As shown in Fig. 12, the ANFIS controller's structure is divided into five layers: the input layer, rule layer, normalisation layer, defuzzification layer and output layer. Here, a and b serve as the ANFIS structure's two inputs, and f serves as its output.

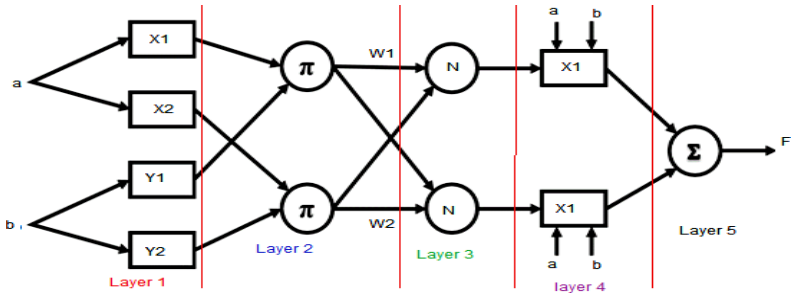

Figure 12. Proposed ANFIS model

The Sugeno FIS-based ANFIS if-then rule configuration is as follows:

Rule 1: if a is X_1 and b isY_1; then $F_1 = t_1 a + u_1 b + v_1$

Rule 2: if a is X_2 and b isY_2; then $F_2 = t_2 a + u_2 b + v_2$

The design parameters for training process are $t_{k,} u_k, v_k$, where $k = 1,2$. The fuzzy sets are represented by the terms X_1 and Y_1.

In the initial layer, the membership functions for each of the specified input data are developed. The membership functions of the adaptive nodes of this layer are given by,

$$O_{1,k} = \mu_{Gk}(a), \mathrm{k} = 1, 2 \tag{26}$$

$$O_{1,l} = \mu_{Hl}(\mathrm{b}), \mathrm{l} = 1, 2 \tag{27}$$

Here, the membership grades for fuzzy set $(X_1, X_2, Y_1 \, and \, Y_2)$ are represented as $\mu_{G_K}(a)$ and $\mu_{H_l}(b)$.

The second layer consists of circular nodes that are labeled as π. This layer multiplies the input signals as shown in the following mathematical expression.

$$O_{2,k} = w_k = \mu_{Gk}(a) \times \mu_{Hk}(\mathrm{b}), \mathrm{k} = 1, 2 \tag{28}$$

Here, the term w_k specifies the firing strength of node k.

The third layer is the normalization layer, which consists of circular nodes that are labeled as N. The output of the second layer is normalized in this layer, as given below.

$$o_{3,k} = \overline{w}_s = \frac{w_s}{w_1 + w_2}, \mathrm{k} = 1, 2 \tag{29}$$

Here, $\overline{w_l}$ specifies the normalized firing strengths.

The third layer output is simplified in the fourth layer and the result is given by,

$$O_{4,k} = \overline{w_s} f_k = \overline{w_s}(t_k\, g + u_k + v_k), \mathrm{k} = 1, 2 \tag{30}$$

Here, $t_{k,} u_k, v_k$ represent the parameter set and the term $\overline{w_s}$ specifies the output of the third layer. The summing of all the inputs is carried out in the final layer. This layer consists of only one node, which is labeled as $\sum$. The overall result is given as,

$$O_{5,k} = \sum_{k=1}^{2} \overline{w_s} f_k = \frac{w_1 f_1 + w_2 f_2}{w_1 + w_2} \tag{31}$$

Premise and consequent parameters refer to the first- and fourth-layer's parameters respectively. While the parameters of the fourth layer are tweaked using a least squares technique, those of the first layer are tuned using a back propagation approach. These two techniques enhance the system's precision and rate of convergence, which enhances ANFIS's capacity for learning.

Table 1. Specifications for HRES

Parameter name	Value
Module cells	42
Cells in series	18
Parallel modules	4
Voltage at open circuit V_{oc}, V	22
Current in short circuits, A	7.3
Duty ratio of converter	0.51
Mosfet Switch s	IRFP260N
power diode D_0	Ug10XCT
Dm1	Ug10XCT
Dm2	Ug10XCT
C_M	5μF/250V
C_{S1}	5μF/250V
C_{S2}	5μF/250V
N	2.8
C_0	100μF
Capacitance in C_1, 100μF	4.73
Capacitance in C_2, 100μF	9998
Inductance in L_1, mH	0.89
Inductance in L_2, mH	6.4
capacitance C_f, 100μF	648
resistance R_c, ohm	0.032
inductance L_f, mH	0.69
resistance R_f, ohm	0.02

4. Results and Discussion

The proposed work is applied in MATLAB and the consequences are acquired in a most useful way as detailed below.

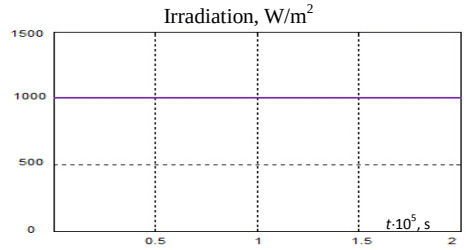

Figure 13. Solar irradiation

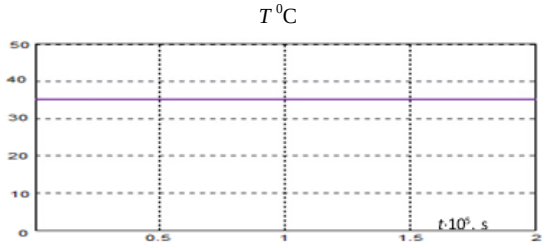

Figure 14. Temperature

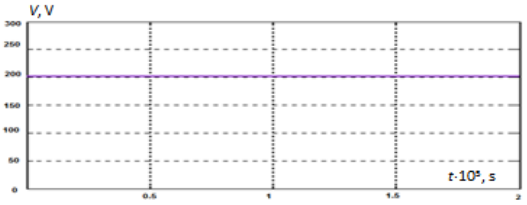

Figure15 (a). PV output voltage

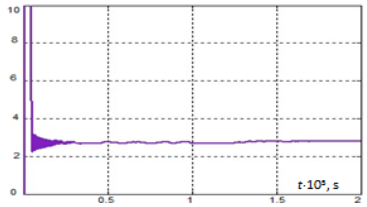

Figure 15 (b). PV output current

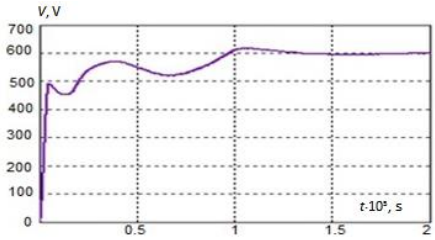

Figure 16 (a). Landsman converter obtained output voltage

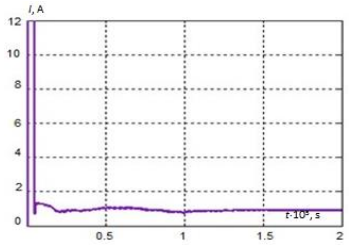

Figure 16 (b). Landsman converter obtained output current

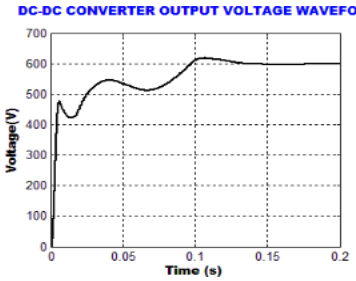

Figure 17. Output voltage of M-SEPIC converter

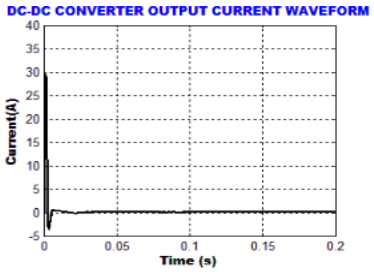

Figure 18. Output current of M-SEPIC converter

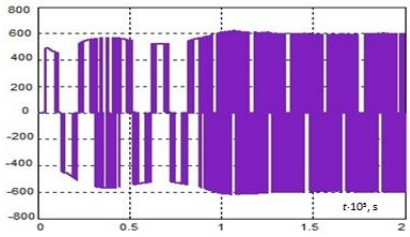

Figure 19(a). Output voltage of VSI

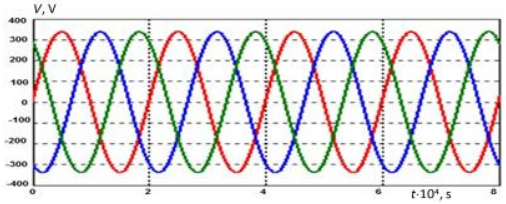

Figure 19(b). Output voltage of (a) VSI

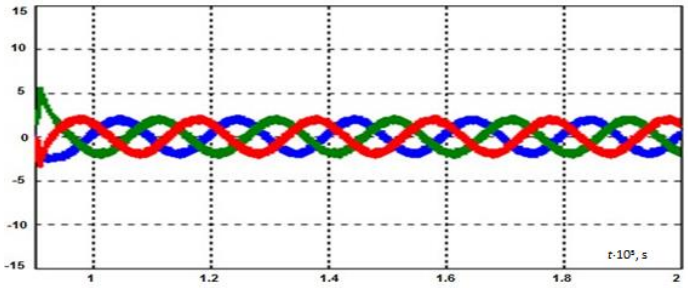

Figure 20. Output current for Grid

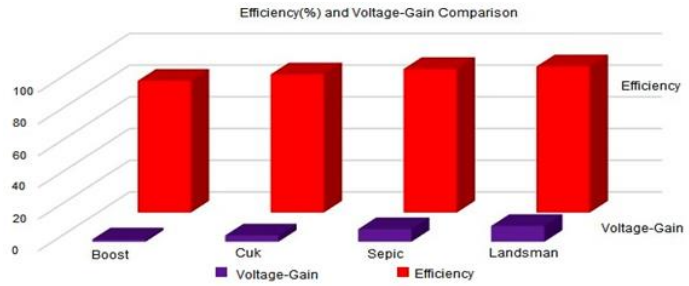

Figure 21. Efficiency and voltage gain of DC-DC converters

The monitoring efficiency of the proposed MPPT set of rules is exposed to be more powerful when analogized with traditional algorithms generally Peturb-Observe (P-O), Incremental Conductance (IC) and fuzzy. The monitoring performance of P-O set of rules, IC, fuzzy and ANFIS are practically as 82 %, 84 %, 88 % and 93 % respectively.

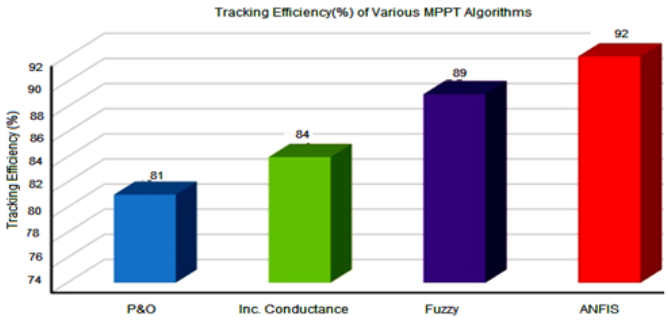

Figure 22. Tracking efficiency of various controllers

5. Hardware Design

The experimental results were obtained with a digital oscilloscope DS1102E 100MHZ [1Gsa/s] and a current amplifier TCP312A with a probe SC1-013-030(100 MHz), PV module BPSX150, dspic30f2010, and 28pin digital signal controller. For isolation purposes, regulator LM317, a three terminal positive adjustable regulator, and opt couplers PC8174 and 4N35IC were employed. The converter with magnetic coupling and a suggested voltage multiplier, and working with a resistive load of 100w have produced the results that are shown. The findings of the experiment resemble theoretical waveforms.

Figure 23. Design of the proposed L-Converter

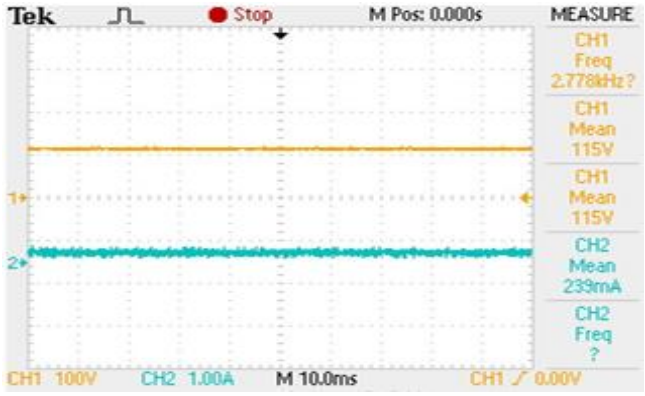

Figure 24. Output voltage and current of the proposed converter

6. Conclusion

Power electronic primarily based DC-DC converters using control circuit with low cost are proposed for photovoltaic system. The advanced DC-DC converters are utilized in this work alongside the neuro fuzzy interface system, for monitoring the most power from photovoltaic device. The converters preserve constant photovoltaic output voltage without thinking about the radiance level. Modified SEPIC converter with magnetic combination is the most superior system with a purpose to gain a very excessive static gain for low input voltage and high output voltage applications. Insertion of voltage multiplier cellular at the secondary side will no longer affect the complication of converter. Moreover, it enhances the converter static benefit. The commutation losses of the suggested converter with magnetic combination, are condensed because of the continuation of the transformer leakage inductance. The major benefit of modified SEPIC converter circuit is that it has a well-known advantage for a given obligation cycle. The Landsman converter presents better results with most performance of 92%, and static gain of 10, and the entire harmonic distortions are minimized to 4%. The proposed work has been tested through simulation/MATLAB software program.

7. Future Scope

The proposed topology can be enhanced to discover utility in structures with low input and excessive output voltage. This topology also can be carried out within the packages which require decreased losses, high strength density, low weight, and quantity. For the reason that machine uses renewable strength supply, it can be efficaciously utilized in extensive range of programs, which includes the UPS device.

References

[1] Gw-Gigawatt, Central electricity authority, International Renewable energy agency,MNRE, India brand equity foundation,Feb 2022.

[2] Mbungu, Nsilulu & Bansal, Ramesh & Naidoo, Raj & Miranda, V. & Bipath, M. (2018). an optimal energy management system for a commercial building with renewable energy generation under real-time electricity prices. Sustainable Cities and Society.41,392-404. DOI:https://doi.org/10.1016/j.scs.2018.05.049

[3] R. M. Elavarasan et al., "A Comprehensive Review on Renewable Energy Development, Challenges, and Policies of Leading Indian States With an International Perspective," in IEEEAccess,vol.8,pp.74432-74457,2020.

[4] Ranjay Singh, Ramesh C. Bansal, Arvind R. Singh, Raj Naidoo. (2018). "Multi-Objective Optimization of Hybrid Renewable Energy System Using Reformed Electric System Cascade Analysis for Islanding and Grid Connected Modes of Operation", IEEE Access, 6, pp 47332 - 47354 Doi: 10.1109/ACCESS.2018.2867276.

[5] Ligade Gitanjali Vasant, V. R. Pawar. (2017). "Solar-wind hybrid energy system using MPPT", 2017 International Conference on Intelligent Computing and Control Systems (ICICCS), 8.

[6] Olubayo Moses Babatunde, Josiah Lange Munda; Yskandar Hamam. (2020). "A Comprehensive State-of-the-Art Survey on Hybrid Renewable Energy System OperationsandPlanning", IEEEAccess, 8, 75313-75346.

[7] Saptarshi De, Gnana Swastika, O. V., Nilanjan Tewari, Anantha Krishnan Venkatesan, Umashankar Subramanian, Mahajan Sagar Bhaskar, Sanjeevikumar Padmanaban, Zbigniew Leonowicz, Massimo Mitolo. (2020). "Implementation of Designed PV Integrated Controlled Converter System", IEEE Access, 8, 100905 - 100915.https://doi.org/10.1109/ ACCESS.2020.2997405

[8] Md Waseem Ahmad, Naga Brahmendra Yadav Gorla, Hasmat Malik, Sanjib Kumar Panda. (2021). "A Fault Diagnosis and Post fault Reconfiguration Scheme for Interleaved Boost Converter in PV-Based System", IEEE Transactions on Power Electronics, 36(4), 3769 - 3780.DOI:https://doi.org/10.1109/TPEL.2020.3018540

[9] Raghavendra, Kummara Venkat Guru, Kamran Zeb, Anand Muthusamy, T. N. V. Krishna, Kumar S. V. S., Do-Hyun Kim, Min-Soo Kim, Hwan-Gyu Cho, and Hee-Je Kim. (2020). "A comprehensive review of DC–DC converter topologies and modulation strategies with recent advances in solar photovoltaic systems", Electronics, 9(1), 31. DOI: https://doi.org/10.3390/electronics9010031

[10] Nathan, K., Ghosh, S.S., Siwakoti, Y.P., & Long, T. (2019). A New DC–DC Converter for Photovoltaic Systems: Coupled-Inductors Combined Cuk-SEPIC Converter. *IEEE Transactionsonnergyonversion, 34*, 191-201.

[11] Ratnakar Babu Bollipo, Suresh Mikkili, Praveen Kumar Bonthagorla, (2021). "Hybrid, optimal, intelligent and classical PV MPPT techniques: A review", CSEE Journal of Power and Energy Systems, 7, 9 - 33.DOI: 10.17775/CSEEJPES.2019.027.

[12] Saeed H. Hanzaei, Saman A. Gorji, Mehran Ektesabi. (2020). "A Scheme-Based Review of MPPT Techniques With Respect to Input Variables Including Solar Irradiance and PV Arrays'Temperature",IEEEAccess,Volume:8,pp:182229-182239.DOI:10.1109/ACCESS.2020.3028580

[13] Amjad Ali, Khalid Almutairi, Sanjeevikumar Padmanaban, Vineet Tirth, Salem Algarni Kashif Irshad;Saiful Islam, Md. Hasan Zahir, Md. Shafiullah, Muhammad Zeeshan Malik. (2020). "Investigation of MPPT Techniques under Uniform and Non-Uniform Solar Irradiation Condition–A Retrospection", IEEE Access, 8, 127368 - 127392.DOI:10.1109/ACCESS.2020..3028580

[14] Mahmud Dhimish. (2019). "Assessing MPPT Techniques on Hot-Spotted and Partially Shaded Photovoltaic Modules: Comprehensive Review Based on Experimental Data", IEEE Transactions on Electron Devices, 66(3), 1132 - 1144.

[15] Shoaib, Muhammad, Imran Siddiqui, Shafiqur Rehman, Shamim Khan, and Luai Alhems, M. (2019). "Assessment of wind energy potential using wind energy conversion system", Journal of cleaner production, 216, 346-360.

[16] Bensalah, Benhamida, A., M. A., Barakat G. and Amara, Y. (2018). "Large wind turbine generators: State-of-the-art review", In 2018 XIII International Conference on Electrical Machines (ICEM), IEEE, 2205-2211.

[17] Ifte Khairul Amin and Mohammad Nasir Uddin. (2020). “Nonlinear Control Operation of DFIG-Based WECS Incorporated With Machine Loss Reduction Scheme”, IEEE Transactions on Power Electronics, 35(7), 7031 - 7044.

[18] Nikolaos Jabbour, Evangelos Tsioumas, Christos Mademlis, Evgeny Solomin, (2020). “A Highly Effective Fault-Ride-Through Strategy for a Wind Energy Conversion System with a Doubly Fed Induction Generator”, IEEE Transactions on Power Electronics, 35(8), 8154 - 8164.

[19] Elsie F. Swana, Wesley Doorsamy. (2019). “Investigation of Combined Electrical Modalities for Fault Diagnosis on a Wound-Rotor Induction Generator”, IEEE Transactions on Power Electronics, 7, 32333 - 32342.

[20] Attapong Mamen, Uthane Supatti. (2017). “A survey of hybrid energy storage systems applied for intermittent renewable energy systems”, 2017 14th International Conference on Electrical Engineering/Electronics, Computer, Telecommunications and Information Technology (ECTI-CON).

[21] M. M. Haji-Esmaeili, E. Babaei and M. Sabahi, "High Step-Up Quasi-Z Source DC–DC Converter," in IEEE Transactions on Power Electronics, vol. 33, no. 12, pp. 10563-10571, Dec. 2018, Doi: 10.1109/TPEL.2018.2810884